

# Xenognosin sensing in virulence: is there a phenol receptor in *Agrobacterium tumefaciens*?

AM Campbell<sup>1\*</sup>, JB Tok<sup>2\*</sup>, J Zhang<sup>2</sup>, Y Wang<sup>2</sup>, M Stein<sup>1</sup>, DG Lynn<sup>2</sup> and AN Binns<sup>1</sup>

**Background:** The mechanisms of signal perception and transmission in the 'two-component' autokinase transmitters/response regulators are poorly understood, especially considering the vast number of such systems now known. Virulence induction from the tumor-inducing (Ti) plasmid of *Agrobacterium tumefaciens* represents one of the best understood systems with regard to the chemistry of the activating signal, and yet the existing data does not support a receptor-mediated perception event for the xenognotic phenols.

**Results:** Here we provide the first conclusive evidence that a specific receptor must be involved in xenognotic phenol perception, detail structural requirements of the xenognosins necessary for perception by this receptor, and develop a genetic strategy that demonstrates critical components of the phenol recognition system are not encoded on the Ti plasmid.

**Conclusions:** Although the basic elements of the two-component system required for phenol-mediated induction of virulence gene expression are encoded on the Ti plasmid, they are dependent on the chromosomal background for even the very first stage of signal perception. This discovery suggests a curious evolutionary history, and also provides functional insight into the mechanisms of two-component signal detection and transmission in general.

## Introduction

*Agrobacterium tumefaciens* is the only known organism that routinely mediates inter-Kingdom gene transfer [1–3], and, as such, has been exploited as a natural vector for the incorporation of foreign genes into higher plants [4]. Briefly, when virulent *A. tumefaciens* infects a wound site, the virulence (*vir*) genes on the resident tumor-inducing (Ti) plasmid are expressed. Their activities result in the production of both the DNA intermediate that will be transferred, and the membrane-bound DNA transfer machinery. The expression of the *vir* regulon is controlled by *virA* and *virG*, two genes homologous to the 'two-component' regulatory systems that are utilized in many bacteria to respond appropriately to environmental signals [5–9]. In this case, VirA serves as the membrane-localized histidine autokinase transmitter (sometimes referred to as 'sensor kinase') and VirG as the response regulator. When the appropriate host recognition factors (xenognosins) are produced and accumulate at the wound site, VirG becomes phosphorylated and the expression of all the *vir* genes, including *virA* and *virG*, are upregulated.

The mechanism(s) that couple transmitter kinase activity to input (signal) control in two component systems remain largely unknown [10,11], and physical data on signal recognition is scant, considering the vast numbers of systems described so far. Within the known two-component

Addresses: <sup>1</sup>Plant Sciences Institute, University of Pennsylvania, Philadelphia, PA 19104-1018, USA. <sup>2</sup>Searle Chemistry Laboratory, 5735 Ellis Avenue, The University of Chicago, Chicago, IL 60637, USA.

\*These authors contributed equally.

Correspondence: DG Lynn; AN Binns  
E-mail: d-lynn@uchicago.edu;  
abinns@mail.sas.upenn.edu

**Key words:** signal transduction, *virA*, *virG*, *vir* gene induction, xenognotic phenol recognition

Received: 23 August 1999  
Revisions requested: 14 September 1999  
Revisions received: 15 October 1999  
Accepted: 19 October 1999

Published: 21 December 1999

**Chemistry & Biology** 2000, 7:65–76

1074-5521/00/\$ – see front matter  
© 2000 Elsevier Science Ltd. All rights reserved.

systems, signal recognition by the transmitter kinase can be either direct or indirect, and the effect of signal recognition at a structural and mechanistic level is not, in general, understood. In the case of VirA/VirG, signal input through VirA is quite complex. Several different classes of xenognotic signals produced at the wound site, including pH, sugars, and phenolics, are recognized and synergistically control *vir* gene expression. The low pH requirement can be altered by mutations within VirA [12,13], but the actual recognition site has not been defined. Monosaccharides, including glucose and arabinose, interact with a chromosomally encoded sugar binding protein, ChvE [14,15], and this complex affects the sensitivity, specificity and maximal response of the system to certain phenols [14–18]. Point mutations or deletions in the periplasmic domain of VirA, both in the putative ChvE binding site and distal to it, can abolish the ability of VirA to respond to sugars [14–18].

Xenognotic phenol recognition is the critical step in VirA/VirG activation. Although VirA is the critical transmitter kinase of phenol-mediated *vir* gene activation, the nature of the perceiving element has not been defined conclusively. Molecular genetic studies of VirA indicate that the linker/kinase domain is the smallest fragment that can function in phenol-mediated *vir* gene expression [19]. Consistent with a role in phenol perception, point mutation [20] within and deletion of the linker domain eliminates the

response to phenols [21,22]. Although genetic studies appeared to indicate that the specificity of the phenols involved in induction is defined by the resident Ti plasmid [23], more recent work [24] indicates that the spectrum of phenols recognized by the system is determined by the relative abundance of both ChvE and the inducing sugars. Finally, deletion of, or point mutations in, the receiver domain of VirA can also increase the range of phenols that are able to induce *vir* gene expression [22].

Beyond the fact that the genetic basis of the phenol specificity in the *Agrobacterium vir* inducing system is not clear, evidence for a specific physical interaction between VirA and the xenognostic phenol has not been presented. In fact, affinity labelling and affinity chromatography approaches to identify specific phenol-binding proteins in *Agrobacterium* have, instead, identified a few small proteins that are not encoded on the Ti plasmid [25,26]. Genetic data indicating the involvement of these proteins in *vir* gene expression has not been obtained, however. These seemingly conflicting data, and the fact that more than 80 different phenols are perceived by *Agrobacterium* and induce *vir* gene expression, raises further questions as to whether there could be a specific receptor. For example, there could be a more general physical manifestation of phenol exposure that controls the response. Here, we develop a combination of chemical and genetic approaches that have made it possible to formally address the question of whether there are specific xenognostic phenol receptors for virulence induction in *Agrobacterium*.

## Results

### Stereochemical evaluation of xenognostic phenols

Although several structural regions of the xenognostic phenols are known to be critical for activity [27–29], only one of the known inducers is chiral, the aglycone of the plant cell growth promoting dehydrodiconiferyl glucoside (DCG) [30–34]. In initial attempts to address the chiral

dependence at this position, the limits of substitution at the benzylic chiral center were evaluated by testing the capacity of the analogs listed in Table 1 to induce expression of a *virE::lacZ* reporter construct. Little change in *vir* gene expression was observed when the alkyl substituent was changed from –H to –CH<sub>3</sub>. Both the maximal induction was reduced and half-maximal effective concentration was increased, however, as the benzylic center was changed from 2° to 3°, to an inactive 4° carbon. Importantly, these structural changes resulted in no significant alteration in the p*K*<sub>a</sub> of the phenol or the required assay conditions, demonstrating that sterically-demanding substituents at this center critically compromise the inducing activity of the phenol.

Given these structural requirements on substituents at the *para* alkyl center, the stereospecificity of the DCG aglycone, DCA, was examined by analysis of the more readily prepared (±)-*trans*-dehydroferulate dimethylester (DDF; Figure 1). Oxidative dimerization of methyl ferulate gave the desired carbon skeleton and the two *trans*-DDF enantiomers were resolved by chiral high-performance liquid chromatography (HPLC). The absolute stereochemistry of each isomer was assigned by conversion to the DCG aglycone [31,35] for which absolute configuration has been assigned [36]. Analysis of the expression of a *virB::lacZ* reporter fusion showed that (2*S*,3*S*)-(–)-*trans*-DDF possessed all the inducing activity of the racemic mixture, at least up to a concentration of 250 μM (Figure 2a). Although this data suggested an absolute stereochemical requirement for *vir* induction, DCA is susceptible to benzofuran ring-opening to the stilbene derivative, a ring-opening expected to be even more pronounced in *trans*-DDF. In fact, mild base treatment of the diester gave the stilbene product a structure that did induce *vir* gene expression under the assay conditions used (data not shown). Attempts to detect the stilbene by HPLC of the bacterial culture during *vir* induction were unsuccessful with both compounds.

**Table 1**

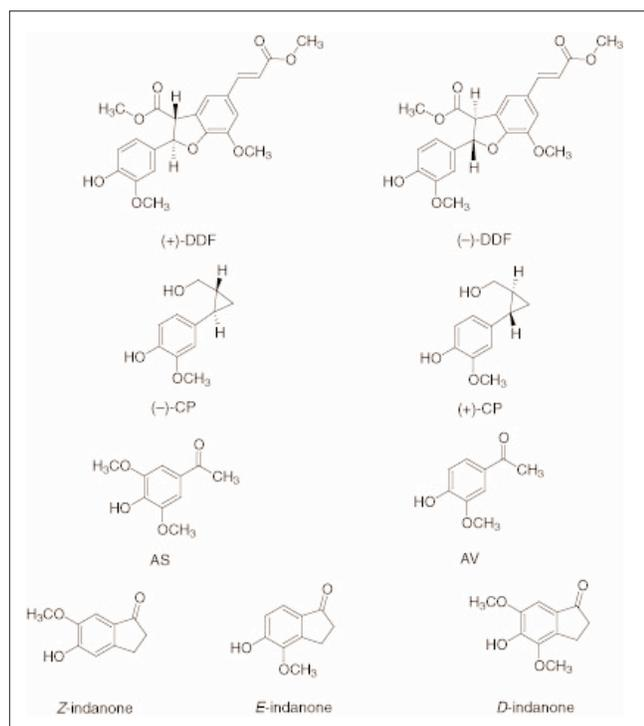
**Effects of benzylic substitution on the p*K*<sub>a</sub> and inducing activity of the guaiacol skeleton.**

Systematic name	R	I <sub>max</sub> (Miller units)	ED <sub>50</sub>	p <i>K</i> <sub>a</sub>
2-Methoxyphenol (Guaiacol)	H	18750	42	9.67
2-Methoxy-4-methyl-phenol	CH <sub>3</sub>	19250	37	9.99
2-Methoxy-4-ethyl-phenol	CH <sub>2</sub> CH <sub>3</sub>	13100	110–120	10.01
2-Methoxy-4-isopropyl	CH(CH <sub>3</sub> ) <sub>2</sub>	8250	220–240	10.01
2-Methoxy-4- <i>t</i> -butyl-phenol	C(CH <sub>3</sub> ) <sub>3</sub>	4250	260–290	10.01

All p*K*<sub>a</sub> values were experimentally determined by monitoring the change in UV absorbance with pH.



Figure 1

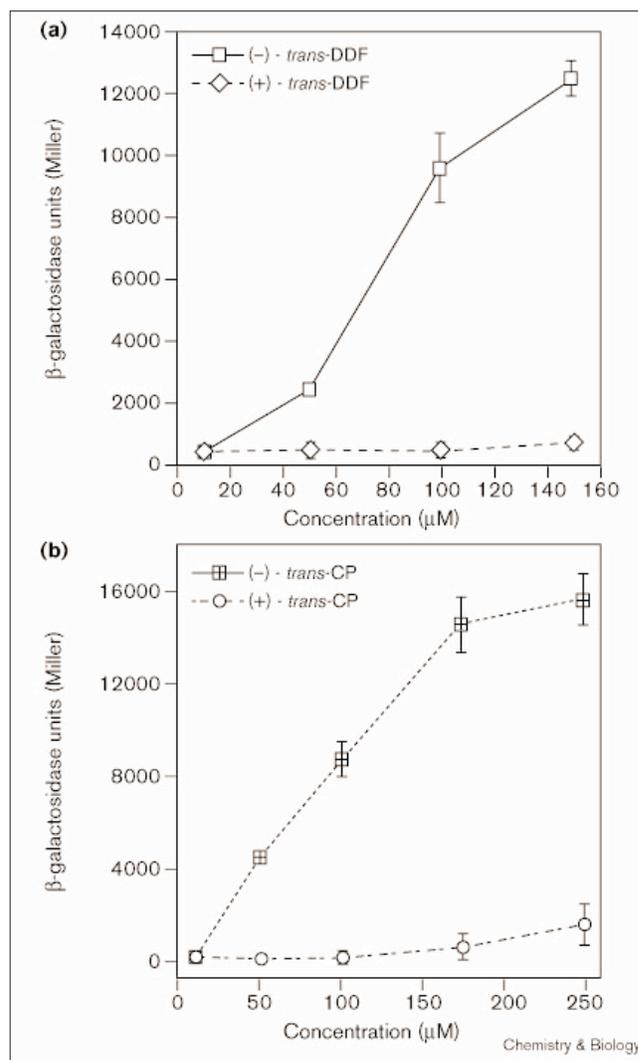


Structural designations.

To address whether stereospecific decomposition to the stilbene accounted for the *vir*-inducing activity, DCA was condensed to the simplest structure that retained the critical phenol for *vir*-inducing activity [27], maintained the three dimensional configuration of the two chiral centers of *trans*-DCA, and suppressed the ring-opening pathway. With the emergence of stereoselective reagents for the construction of chiral three-membered carbocycles [37–43], general routes for the preparation of the appropriate *trans*-cyclopropanes were developed. Both *trans*-isomers and *cis*-isomers were prepared via the appropriately substituted styrene, ethyl diazoacetate and the bis[(4*S*)-oxaline] copper (II) catalyst [40,41]. The predicted isomers, (1*R*,2*R*)-*trans*-1-hydroxymethyl-2-(4-hydroxy-3-methoxyphenyl)-cyclopropane (*trans*-CP; Figure 1) and (1*S*,2*R*)-*cis*-1-hydroxymethyl-2-(4-hydroxy-3-methoxyphenyl)-cyclopropane (*cis*-CP; Figure 1) were obtained in over 90% enantiomeric excess (ee) as determined by chiralcel OD HPLC.

Confirmation of the absolute stereochemical assignment was obtained using both coupled oscillator analysis of the dibenzoates [44,45] of the *trans*-CP isomers as well as an alternate enantioselective synthesis. Charrette *et al.* [46,47] and Theberge *et al.* [48] have demonstrated predictable stereoselective cyclopropanation using dioxaboralane enantiomers as directing groups in the Furukawa

Figure 2

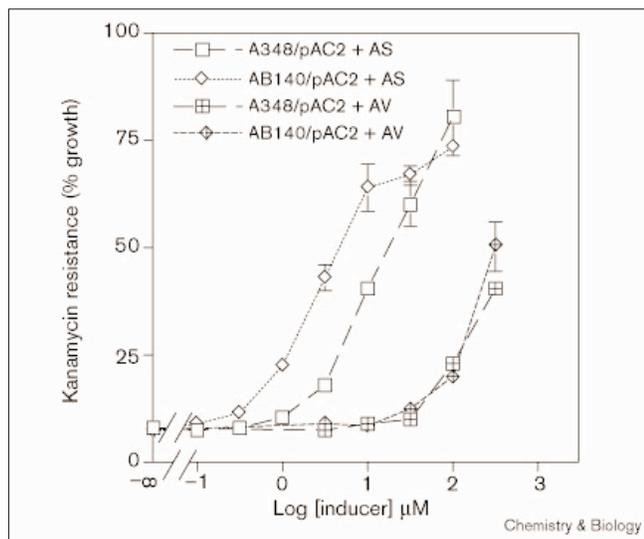


Induction of *vir* expression.  $\beta$ -Galactosidase expression in A348 carrying pSW209 (*virB::lacZ*) induced with (a) (-)-*trans*-DDF, (+)-*trans*-DDF, and (b) (+)-*trans*-CP and (-)-*trans*-CP. Expressed as mean  $\pm$  standard deviation ( $n = 3$ ).

reaction [49–52]. Cyclopropanation of the protected *trans*-4-benzyloxy-3-methoxy cinnamyl alcohol via this strategy indeed resulted in the efficient, enantioselective (89%–92% ee) preparation of *trans*-CP isomers, further establishing the absolute stereochemical assignment.

Each of the *cis* and *trans* enantiomers of CP were tested for their ability to induce *vir* gene expression. In the case of *cis*-CP, the (+) and (-) enantiomers showed equivalent activity (data not shown). The chiralcel OD purified (+)-*trans*-CP, however, accounted for virtually all the activity of the *trans* racemate (Figure 2b). Significantly, the three-dimensional arrangement of the substituents on the cyclopropyl centers of the active (+)-*trans*-CP are identical to both the active

Figure 3



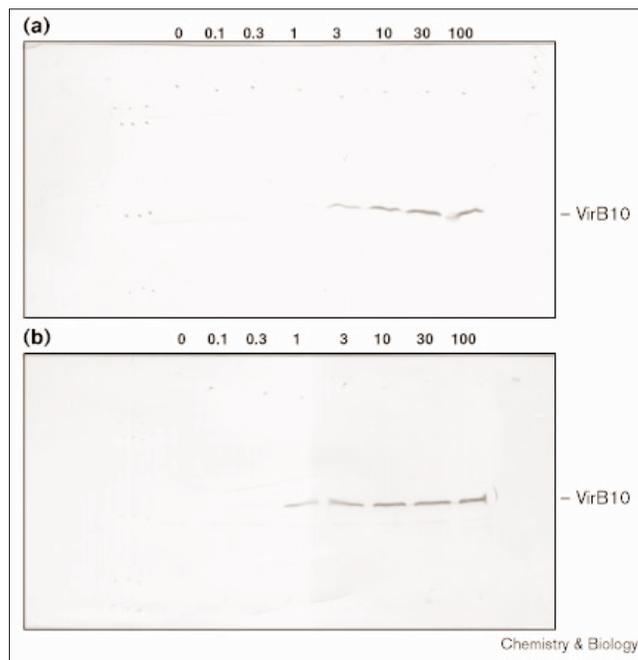
Cell growth. Kanamycin-resistant growth of wild-type A348 and AB140, each carrying pAC2 (*virB<sup>npII</sup>*), expressed as a percentage of control with AS induction in wild-type A348/pAC2, AV in wild-type A348/pAC2, AS in AB140/pAC2, and AV in AB140/pAC2. Expressed as mean  $\pm$  standard deviation ( $n = 3$ ).

DCA and DDF, in which the ester replaces the hydroxymethyl substituent, isomers. The cyclopropyl ring is also significantly more stable to ring-opening than the benzofuran of either DDF or DCA. These results demonstrate that chiral specificity at centers distant to the OH can be critical in phenol-mediated induction of *vir* gene expression, and provide support for the hypothesis that a specific receptor, or receptors, must be involved in signal perception.

#### Isolation of AS hypersensitive mutants

To evaluate further the implicated specific phenol receptor that mediates expression of the virulence genes in *Agrobacterium*, a new genetic screen was devised to isolate mutants with altered inducer sensitivity. A broad-host-range plasmid containing the neomycin phosphotransferase (*npII*) gene under the control of the *virB* promoter [53], pAC2, was constructed. This plasmid confers on the wild type *A. tumefaciens* strain A348 the capacity to grow in medium containing kanamycin only when a sufficient concentration of *vir*-inducing phenol is present. The selection strategy was to incubate large numbers of A348/pAC2 cells on agar solidified plates containing IM, 40  $\mu\text{g/ml}$  kanamycin and 10  $\mu\text{M}$  AS, a concentration that is tenfold lower than is required by these cells to survive in the presence of kanamycin. Two classes of surviving colonies were recovered, constitutive and hypersensitive mutants, easily distinguished by patching the colonies onto medium containing kanamycin but lacking AS. Using this strategy, nine hypersensitive mutants were isolated from a total of greater than  $2 \times 10^7$  cells exposed to the selection conditions.

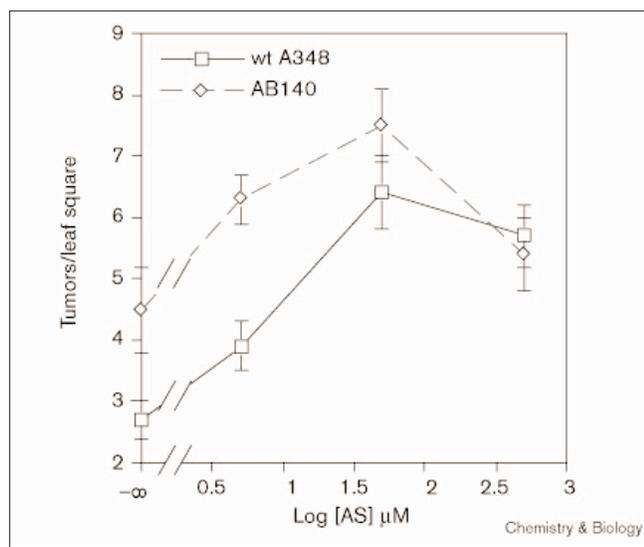
Figure 4



Expression of *virB10*. Immunoblot analysis of AS induction in (a) wild-type A348 and (b) AB140 with anti-VirB10 antibody following induction with the indicated concentration of AS (in  $\mu\text{M}$ ).

The hypersensitive nature of the mutants was confirmed by evaluating their dose response to AS. For example, mutant AB140 was tested for kanamycin resistance in liquid medium over a range of AS concentrations. As shown in Figure 3, AB140 grows in the presence of kanamycin at approximately one-half log lower concentration of AS than does wild type. AB140 shows no basal level induction of *vir* gene expression, as judged by growth in kanamycin-containing medium in the absence of AS, demonstrating that this is not a constitutive mutant. Intriguingly, this mutant, and all others tested thus far, are not hypersensitive to monomethoxyphenols, for example, AV, indicating that the observed change in phenol sensitivity is specific to the dimethoxyphenols.

To ensure that the mutants that were hypersensitive to AS were a result of a change in the *vir* gene induction pathway rather than a mutation in the reporter plasmid pAC2, other methods to analyze *vir* gene induction and the virulence response were investigated. First, all nine mutants were transformed with pSW209 carrying a *virB::lacZ* reporter construct. The  $\beta$ -galactosidase activities of all strains were hypersensitive in an AS dose-response experiment (data not shown). The observed changes are not because of some artifact of the reporter plasmids as the expression of VirB10, one of the proteins of the *virB* operon on its Ti plasmid, in cells of AB140 was detectable after induction with 0.3  $\mu\text{M}$  AS (Figure 4).

**Figure 5**

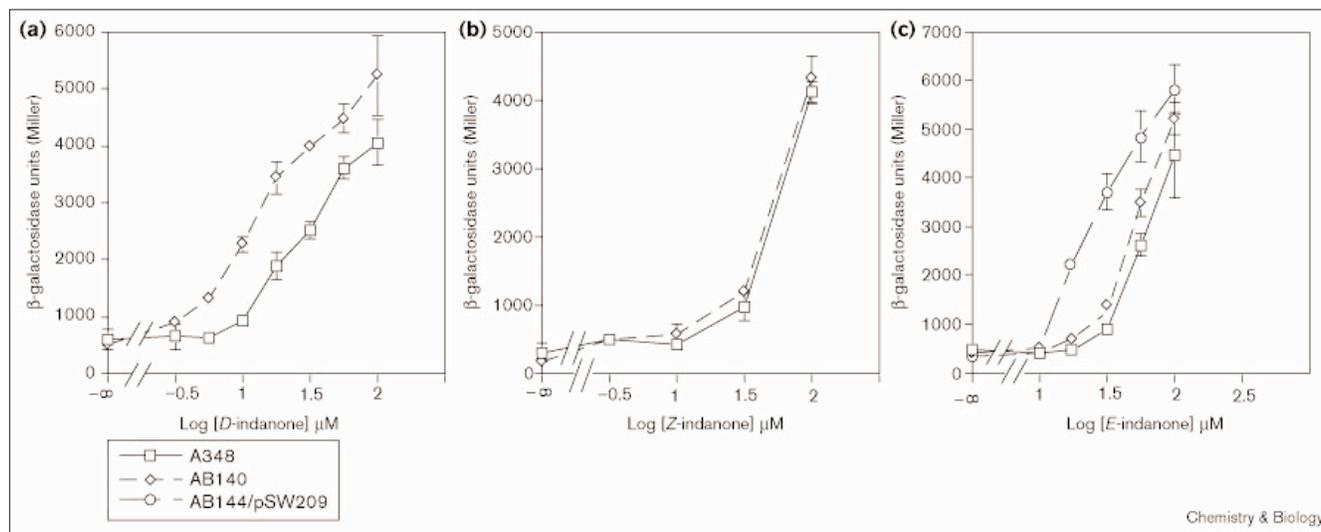
Tumor induction. Tobacco leaf square pieces were co-cultivated with wild-type A348 and AB140 in the presence of various concentrations of AS. After 12 days, the leaf pieces were scored for the mean number of tumors per leaf square  $\pm$  standard error ( $n = 20$ ).

Wild-type cells required 1  $\mu\text{M}$  AS to produce detectable VirB10. Thus, the mutants are hypersensitive to AS when assaying either the *virB<sup>P</sup>/nptII* reporter, the *virB::lacZ* reporter, or directly assaying expression of VirB10 from the native *virB* promoter on the Ti plasmid. These results demonstrate that the mutation affects some aspect of the phenol-mediated induction of *vir* expression.

A crucial question is whether or not the mutants that demonstrate hypersensitivity to the xenogonistic phenols are also ‘hypervirulent’. The virulence of the strains was assayed by monitoring their capacity to induce crown gall tumors in the tobacco leaf assay. In this assay, bacteria and leaf explants are co-cultivated for two days at varying levels of AS and then transferred to antibiotic-containing medium that stops bacterial growth but allows plant tumor growth [16]. In the case of wild-type strain A348, some tumor formation is observed on the leaf explants co-cultivated in the absence of AS in the co-cultivation, as expected because of xenogonistic phenols released from the wounded cells (Figure 5). As the concentration of the phenol in the co-cultivation medium was increased, the number of tumors formed per infected leaf explant significantly increased. The hypersensitive mutant AB140 induced significantly more tumors than wild type in the absence of AS in the co-cultivation medium, and, most importantly, reached its maximal capacity to induce tumors at a log order lower concentration of AS in the co-cultivation medium (Figure 5). Importantly, the maximum number of tumors formed by both the wild-type strain and AB140 was approximately the same, consistent with the observation that the hypersensitivity of AB140 is not a result of simple overexpression of the *vir* genes. Thus, the hypersensitive response for *vir* expression demonstrated using the reporter assay is matched by ability of AB140 to induce tumor formation at low concentration of xenogonin.

#### Structural specificity

The selected mutants exhibited the same stereospecificity as the wild-type strain. The (+)-*trans*-CP accounted for all the inducing activity of the racemate and the

**Figure 6**

Induction of *vir* expression.  $\beta$ -Galactosidase induction with (a) *D*-indanone, (b) *Z*-indanone, and (c) *E*-indanone in wild-type A348, AB140 and AB144 carrying pSW209 (*virB::lacZ*). Mean  $\pm$  standard deviation ( $n = 3$ ).

mutants appeared at best slightly hypersensitive to the active enantiomer (data not shown). The free rotation of the *para* benzylic substituent in AV, AS, as well as the CP and DDF enantiomers raises the possibility that geometric isomers relating the orientation of that group to the ring methoxy substituent could exist in the receptor-bound xenogonins. To evaluate this possibility, the rotation of the aryl-carbonyl bond was locked via the construction of isomeric indanones. The inducing activity of the 5-hydroxy-4,6-dimethoxyindanone (*D*-indanone) was little changed from AS in a wild-type background, and as with AS, AB140 was hypersensitive to this compound (Figure 6a).

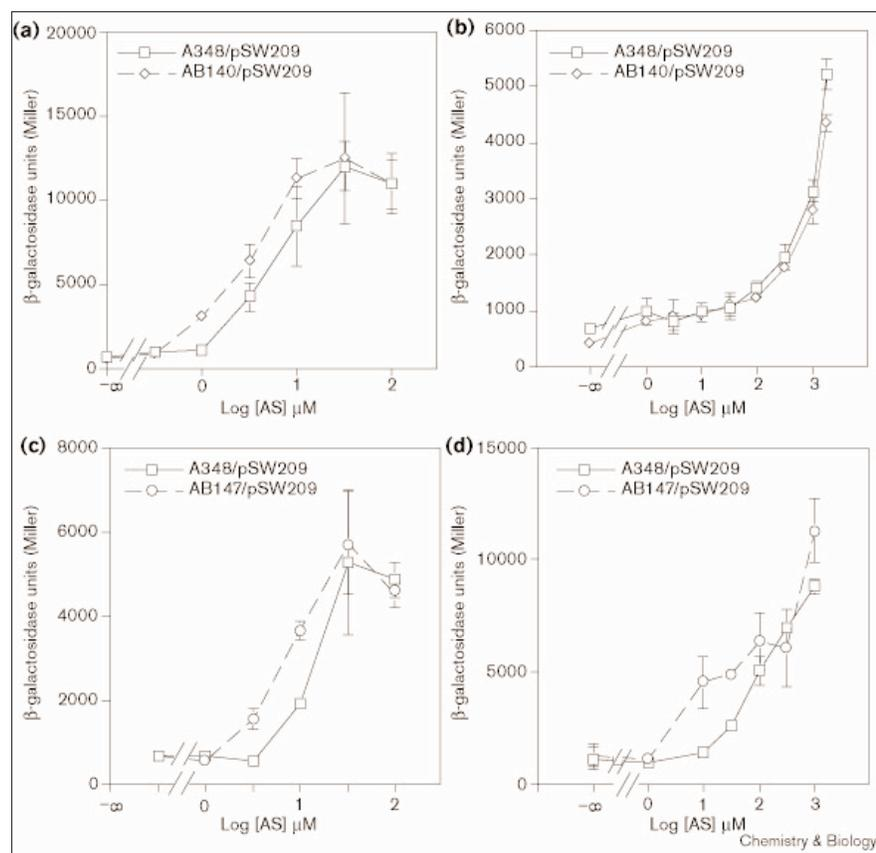
The *E*-indanone, 5-hydroxy-4-methoxyindanone, constrains the carbonyl oxygen and the methoxy on opposite sides of the phenol-alkyl axis, whereas the *Z*-indanone, 5-hydroxy-6-methoxyindanone, positions them on the same side of this axis. Although wild-type strain A348 responds to the isomeric indanones with equivalent activity, AB140 is hypersensitive only to the *E*-indanone (Figure 6b,c). The *E*-indanone does not account for all the hypersensitivity of the *D*-indanone in AB140, but it does so in a second hypersensitive strain, AB144 (Figure 6c). Similar results were observed with strains

AB146 and AB147, all the hypersensitivity of AB146 to the *D*-indanone was accounted for by the *E*-indanone whereas the hypersensitivity of AB147 was only partially accounted for by the *E*-indanone (data not shown). Curiously, only the *E*-indanone was responsible for any of the hypersensitivity in the strains thus far analyzed.

#### Effect of sugars on phenol hypersensitivity

The results of Peng *et al.* [24] demonstrate that both phenol sensitivity and specificity are dramatically affected by the presence of inducing sugars and are attributable to the ChvE-VirA interaction. This result suggests that a possible mechanism for the change in sensitivity and specificity described here exists within the sugar perception and signaling system. The phenol hypersensitive strains were tested in the presence or absence of 0.1% arabinose, and using this analysis the mutants fell into two classes. The first, characterized by strain AB140, exhibits a sugar-dependent hypersensitive phenotype (Figure 7a,b). Only when arabinose was present in the induction medium was the sensitivity to AS increased in comparison with wild type strain A348. The second class of mutants, characterized by strain AB147, exhibits a sugar-independent hypersensitive phenotype (Figure 7c,d). Even in the absence of arabinose,

Figure 7



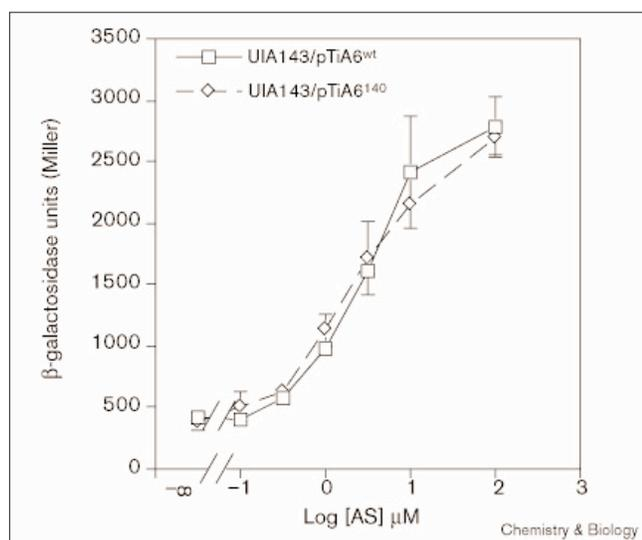
Induction of *vir* expression.  $\beta$ -Galactosidase induction in strains grown at varying AS concentrations in ABIM plus 1% glycerol in the (a,c) presence or (b,d) absence of 0.1% arabinose. (a,b) A348/pSW209 and AB140/pSW209, (c,d) A348/pSW209 and AB147/pSW209. Mean  $\pm$  standard deviation ( $n = 3$ ).

these strains are hypersensitive to AS, responding to AS at a half log lower concentration than does the wild-type strain. Typical of this class, AB147 is more sensitive to AS in the presence of arabinose than in its absence (Figure 7c,d), indicating that they still are responding to the ChvE–sugar signaling system.

### Genetic characterization

To determine whether the gene responsible for phenol hypersensitivity of the mutants was *virA* or was located on the Ti plasmid, the Ti from both wild-type A348 and the mutants were moved into strain UIA143 by conjugation. UIA143 has the same chromosome as both A348 and the mutants but lacks a Ti plasmid. Transconjugants carrying either the wild-type pTiA6 or Ti of AB140 responded identically to AS for *vir* induction (Figure 8). The Ti plasmids of five additional hypersensitive mutants, both sugar independent and sugar dependent, were conjugated into UIA143, and in all cases, the transconjugants exhibited wild-type sensitivity to the xenognostic phenols. These results indicate that mutations in *virA* are not responsible for the hypersensitive phenotype, and, additionally, demonstrate that no other gene localized to the Ti plasmid, including *virG*, is responsible for the phenotype. The only other gene known to be critical in the phenol induction pathway is *chvE*. Sequence analysis revealed, however, that *chvE* genes from both sugar-dependent and sugar-independent strains are also wild-type (data not shown). The gene responsible for the phenol hypersensitive phenotype must, therefore, be a new component in the xenognosin response system.

**Figure 8**



Induction of *vir* expression. Ti plasmids of wild-type A348 and AB140 were conjugated into UIA143/pSW209 and  $\beta$ -galactosidase expression was measured in UIA143/pTiA6<sup>wt</sup> and UIA143/pTiA6<sup>140</sup>. Mean  $\pm$  standard deviation ( $n = 3$ ).

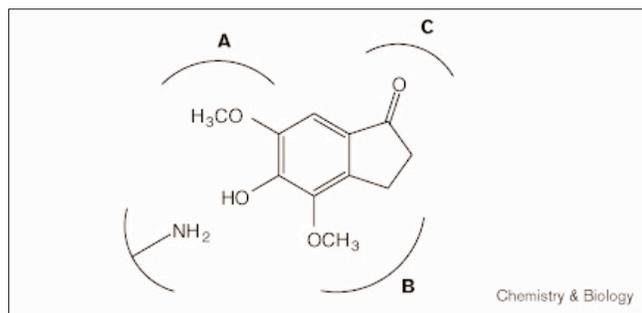
### Discussion

More than 80 different phenols are able to induce virulence in *A. tumefaciens*, and this broad structural diversity might be best explained by a *vir* induction mechanism that exploits a general physical effect of the phenol rather than perception through a specific receptor. The findings that only a single enantiomer of the chiral inducers, (–)-*trans*-DDF and (+)-*trans*-CP, are active; that the three-dimensional arrangements of the substituents on these molecules are identical; and that no stereospecific metabolism or uptake of the different chiral isomers could be detected, argue that indeed an enantiospecific receptor must exist.

Further proof for the existence of this receptor(s) was found by constructing pAC2, which carried a *npfII* gene under the control of the *virB* promoter. This plasmid offered a new selection strategy in which survival in kanamycin-containing medium at low AS concentrations could only occur in mutants that either had increased sensitivity to AS or were constitutive for *vir* gene expression. Earlier genetic strategies to search for mutations in the *A. tumefaciens* xenognosin recognition system utilized approaches that screened potential mutants for either suppression of virulence and/or *vir::lacZ* fusion expression [20,54,55], or up-regulation of *vir::lacZ* expression in the absence of xenognostic phenols [22,56–58]. In these cases, mutations were generated either by transposon mutagenesis, which would completely disrupt the gene and cause polar mutations, or targeted mutagenesis of the expected receptor, *virA*. In contrast, our strategy provides a selection scheme that can be used to search for mutations affecting phenol-mediated *vir* gene expression throughout the *A. tumefaciens* genome. The isolation of mutants that demonstrate a xenognostic phenol-specific hypersensitivity demonstrates the power of this strategy and will ultimately facilitate cloning the responsible gene(s).

To the extent that the differential responsiveness of the *vir* gene expression system to the xenognostic phenol can be attributed to differences in receptor affinity, a model for the binding interaction can be developed (Figure 9). A critical primary amine is placed proximal to the phenolic OH for the proton-transfer activation [25,27,59]. The *ortho* methoxy groups must contribute positively and equally to the binding affinity in the wild-type receptor, but in the mutants, domains A and B cannot be equivalent. In all of the mutants obtained thus far, it is both the interaction between the methoxy group and the domain B that contributes significantly to the hypersensitivity. The observation that the *E*-indanone, but not AV, is more effective at inducing *vir* gene expression in the hypersensitive mutants establishes that the alkyl substituent also contributes to the apparent increased binding affinity of the mutants. The active (+) *trans*-CP enantiomer is only slightly more active than wild type, however, and the methoxy region of the phenol edge appears to be the most critical.

Figure 9



Model of the *D*-indanone receptor. Regions A, B and C represent domains of the Xbp involved in binding.

The phenol hypersensitive mutants are unique in that the new structural requirements of the phenol for maximal sensitivity are not related to *virA* or any other gene on the Ti plasmid. To date the only other protein known to be involved in phenol-mediated induction of *vir* expression is ChvE, a sugar-binding protein that interacts with the periplasmic domain of VirA and increases the sensitivity of the system to phenols. Sequence analysis demonstrates that ChvE is wild type in both sugar-dependent and sugar-independent hypersensitive strains. Although the hypersensitive phenotype is sugar-independent in many cases, these strains continue to demonstrate the normal response to the inducing sugars.

Previous analyses of VirA have suggested that the linker domain functions as a phenol-mediated activator of the VirA/VirG phosphorylation cascade [19–22]. This domain is also critical for the transduction of the ChvE–sugar signal that results in increased phenol sensitivity. The results reported here are consistent with a new model in which the ChvE–sugar interaction with the periplasmic domain of VirA mediates conformational shifts of a hypothetical xenogostic phenol-binding protein (Xpb) that is bound to the linker domain of VirA, thereby increasing the apparent affinity of Xpb for the phenols. In the case of the sugar-dependent hypersensitive mutants, this conformational shift would be required for mutant Xpbs to exhibit altered affinity. In contrast, the sugar-independent mutant Xpbs, although still capable of responding to the ChvE–sugar activation of VirA, can exhibit an increased affinity for the phenols in the absence the ChvE–sugar activation.

Consistent with this model is the data demonstrating that, as with the non-Ti plasmid-localized mutations described here, mutations in either the repressing response-regulatory domain or the periplasmic domain of VirA [22] can increase sensitivity as well as the structural specificity of the xenogostic phenol. Interestingly, no mutations that affect phenol specificity have been observed in the linker domain

of VirA. Taken together, these observations suggest that the linker domain of VirA might serve to integrate signal input, and that the activation barrier for signal response can be reduced by mutations in both VirA and the Xpbs. Formally, the Xpb could serve either to activate the phosphotransfer system when phenols are bound or, alternatively, act as a repressor of the phosphotransfer system, in which case repression would be relieved by phenol binding. This model is also consistent with physical evidence for the existence of chromosomally encoded Xpbs in *Agrobacterium* and explains the inability to obtain any physical evidence for xenogostic phenol-binding to VirA [25,26]. An alternative model is that the hypersensitive phenotype is the result of increased uptake or altered metabolism of the phenolics in question. Although this possibility has not been rigorously excluded, the current results clearly demonstrate the specificity of the alteration and its importance in both *vir* gene expression and virulence.

### Significance

Two-component regulatory systems control many bacterial responses to its environment, as well as a variety of pathogenic processes [5–9]. Genetic analysis indicates that in most two-component-system autokinase transmitters, periplasmic and/or cytoplasmic regions are necessary for signal input whereas in only a few cases, for example, FixL, which binds oxygen at its heme [60,61], has the ligand-binding site been identified. Many membrane-bound transmitter kinases do rely on other proteins for signal recognition. VirA itself requires the ChvE protein for sugar perception [18,62] and recent data on PhoR indicates that the kinase domain requires other proteins to respond appropriately to phosphate starvation [63,64]. Despite the inherent simplicity of the central two-components in these signal transduction chains, the function and evolutionary origin of these accessory proteins and the role they play in the regulation of signal perception and transmission appears quite sophisticated. Continued analysis of these hypersensitive mutants, in particular identifying the protein product responsible for the phenotype and the signal-recognition event(s) mediated by them will contribute greatly in elucidating the biochemistry of signal perception by transmitter kinases in general.

### Materials and methods

Proton ( $^1\text{H}$ ) NMR spectra were either obtained on the University of Chicago DS-1000 spectrometer that was equipped with a Nicolet 1280 data acquisition system operated at 500 MHz, or on a General Electric (GE) QE-300 spectrometer operating at 300 MHz. Carbon ( $^{13}\text{C}$ ) NMR spectra were obtained on a General Electric QE-300 spectrometer operating at 75 MHz. Two-dimensional (2D) NMR spectra were obtained on a GE GN-500 spectrometer that was equipped with the Omega Data system. Low-resolution mass spectra (MS) were obtained using a UG 70-250 mass spectrometer. The HPLC system was a Rainin system that included Model HPXL pumps (pressure module max; 8,700 psi), Dynamax absorbance detector (model UV-D) and a Macintegrator software installed into the MacPlus computer. Ultraviolet (UV)

spectra were recorded with a Perkin-Elmer lambda 6 UV/VIS spectrophotometer in quartz cuvettes with an optical pathway of 1 cm. Circular dichroism (CD) spectroscopy was measured using a Jasco-600 CD spectrophotometer. Optical rotation was measured with a Perkin-Elmer 141 polarimeter. Ozonolysis is carried out with a Welsbach model T-408 laboratory ozonier, Welsbach Corp., Philadelphia, PA.

### Syntheses

Acetosyringone (AS), acetovallinone (AV), guaiacol, 4-methyl-2-methoxyphenol, and 5,6-dimethoxy-1-indanone were either purchased from Aldrich and Lancaster Chemical Companies and were used directly. The syntheses of dehydrodiconiferyl ferulate, 3-(4'-hydroxy-3'-methoxyphenyl)-butan-1-ol, and 2-phenoxy-2-(4'-hydroxy-3'-methoxyphenyl)-ethanol were completed as previously reported by Hess *et al.* [59]. HPLC grade solvents were purchased from Fisher Chemical Company or J.T. Baker Chemical Company. Tetrahydrofuran (THF) and diethyl ether were distilled from sodium/benzophenone and dichloromethane ( $\text{CH}_2\text{Cl}_2$ ) was distilled from calcium hydride.  $\text{H}_2\text{O}$  was double distilled from all glass stills.

Flash column chromatography employed EM Science silica gel, 230–400 mesh, 40–63 Å in diameter. Thin layer chromatography was performed with Baker-flex silica gel IB2-F plastic backed plates with a 0.25 mm silica gel layer. Plates were visualized by 254 nm illumination, and/or treatment with a ceric ammonium sulfate/trichloroacetic acid.

Synthetic methods and structural characterization of 2-methoxy-4-ethylphenol, 2-methoxy-4-isopropylphenol and 4-(tert-butyl)-2-methoxyphenol are described in the Supplementary material section.

*trans-4-Benzoyloxy-3-methoxy cinnamyl alcohol*. *trans-4-Hydroxy-3-methoxy-cinnamic acid* was esterified ( $\text{MeOH}$ ,  $\text{SOCl}_2$ ) and benzylated to afford the methyl *trans-4-benzoyloxy-3-methoxy cinnamate*. A dried three-necked flask equipped with an additional funnel and under  $\text{N}_2$  was charged with lithium aluminum hydride (LAH) suspended in THF and cooled in an ice bath for 15 min before a solution of methyl cinnamate in THF was added dropwise with stirring. After 15 min the reaction mixture was partitioned between EtOAc and dilute aqueous HCl and the organic phase was washed with brine, dried with sodium sulfate, concentrated and chromatographed ( $\text{SiO}_2$ , hexanes: EtOAc, 7:3) to give *trans-4-benzoyloxy-3-methoxy cinnamyl alcohol* as a yellow oil.

(+)- and (-)-*trans-[3-(4-Hydroxy-3-methoxy-phenyl)-cyclopropyl] methanol* (*trans-CP*). The enantiomers of dioxaborolane were prepared by refluxing the corresponding N, N, N', N'-tetramethyl-tartaric acid diamide with 1-butaneboronic acid in anhydrous toluene in a Dean-Stark trap for 15 h. A 100 ml flask charged with 30 ml distilled  $\text{CH}_2\text{Cl}_2$  was cooled to  $-25^\circ\text{C}$  before 8.9 ml (8.9 mmol) of a 1.0 M solution of diethyl zinc in hexanes, 0.93 ml (8.9 mmol) of ethylene glycol dimethyl ether, and 1.43 ml (17.8 mmol) of diiodomethane were added and stirred for 10 min. 0.48 g (1.78 mmol) of the protected cinnamyl alcohol and 0.53 g (1.95 mmol) of the chiral dioxaborolane were added in 10 ml  $\text{CH}_2\text{Cl}_2$ , and the reaction mixture was stirred for 3 h, quenched with 50 ml saturated  $\text{NH}_4\text{Cl}$ , and the aqueous portion was extracted with diethyl ether. The combined organic layers were stirred vigorously for 12 h with aqueous KOH (5 M), and the organic layer was then successively washed with 10% aqueous HCl, saturated aqueous  $\text{NaHCO}_3$ ,  $\text{H}_2\text{O}$ , saturated aqueous NaCl, and dried, concentrated *in vacuo* and chromatographed on  $\text{SiO}_2$  (1:4, hexane/EtOAc) to afford 0.35 g (69%) of the desired cyclopropylmethanol.  $^1\text{H}$  NMR;  $\delta$  ( $\text{CDCl}_3$ ) 7.43–7.30 (m, 5H), 6.78 (d, 2H), 6.65 (d, 1H), 6.56 (dd, 1H), 5.12 (s, 2H), 3.88 (s, 3H), 3.61 (m, 2H), 1.77 (m, 1H), 1.53 (b, 1H), 1.38 (m, 1H), 0.90 (m, 2H);  $^{13}\text{C}$  NMR;  $\delta$  ( $\text{CDCl}_3$ ) 149.5, 146.2, 137.3, 135.6, 128.4, 127.7, 127.2, 117.6, 114.3, 110.2, 71.2, 66.5, 55.9, 24.8, 20.9, 13.3. *Trans-[3-(4-benzoyloxy-3-methoxy-phenyl)-cyclopropyl] methanol* underwent hydrogenolysis to afford after chromatography ( $\text{SiO}_2$ , 1:1, hexane/EtOAc) either (+)- or (-)-*trans-CP*.  $^1\text{H}$  NMR;  $\delta$  ( $\text{CDCl}_3$ ) 6.80 (d, 2H), 6.61 (d, 1H), 6.56 (dd, 1H), 5.57 (s, 1H), 3.59 (m, 2H), 1.77 (m, 1H), 1.65 (b, 1H), 1.38 (m, 1H), 0.88 (m, 2H);  $^{13}\text{C}$  NMR;  $\delta$  ( $\text{CDCl}_3$ ) 149.1, 146.3, 134.1, 118.4, 115.2, 109.0, 66.5, 55.8, 24.6, 21.0, 13.1.

*5-Hydroxy-4-methoxy-1-indanone (E-indanone)*. A 50 ml three-necked flask fitted with a vacuum line, a nitrogen line and a  $\text{H}_2$ -filled balloon was charged with 2,3-dimethoxycinnamic acid (3.0 g; 0.014 mmol), 10% Pd/C catalyst (3 spatula tips) and 20 ml of absolute ethanol was stirred vigorously. The flask was evacuated and flushed with  $\text{N}_2$  three times, filled with  $\text{H}_2$  and after 40 mins the Pd/C catalyst was removed through a short column of celite, and the solvent evaporated *in vacuo* to afford 2,3-dimethoxyphenylpropanoic acid in 97% yield.  $^1\text{H}$  NMR (300 M Hz,  $\text{CDCl}_3$ )  $\delta$  7.01 (d, 1H, J = 7.9 Hz, aromatic), 6.81–6.84 (m, 2H, aromatic), 3.88 (s, 6H, 2  $\text{OCH}_3$ ), 2.99 (t, 2H, J = 7.7 Hz), 2.69 (t, 2H, J = 8.2 Hz). Mass spectrum ( $\text{EI}^+$ , 70 eV)  $m/z$  210 ( $\text{M}^+$ , 100%), 164 (30%), 151 (44%), 136 (46%), 91 (61%), 77 (35%), 65 (24%).

A 1 l beaker containing 50 g of polyphosphoric acid (PPA) was heated over a steam bath to  $90^\circ\text{C}$  before 2,3-dimethoxyphenylpropanoic acid, 2.0 g (9.52 mmol), was added in one portion and stirred vigorously with a glass rod for 3 min (the temperature should remain around  $90^\circ\text{C}$ ). Another 50 g of liquefied PPA was added and the mixture was warmed with vigorous stirring for another 4 min, cooled to  $60^\circ\text{C}$  with 150 g of crushed ice and stirred until a yellow oil has separated. The resulting mixture was extracted 3× with ether, the combined organic fractions washed with 5% NaOH and water, dried over anhydrous sodium sulfate and evaporated *in vacuo* to afford 4,5-dimethoxy-1-indanone as a yellowish oil in 86% yield.  $^1\text{H}$  NMR (300 MHz,  $\text{CDCl}_3$ )  $\delta$  7.51 (d, 1H, J = 8.5 Hz, aromatic), 7.01 (d, 1H, J = 8.6 Hz, aromatic), 6.36 (s, 1H, -OH), 4.02 (s, 3H, - $\text{OCH}_3$ ), 3.98 (s, 3H, - $\text{OCH}_3$ ), 3.08 (t, 2H, J = 6.1 Hz, - $\text{CH}_2$ -), 2.71 (t, 2H, J = 5.8 Hz, - $\text{CH}_2$ -).  $^{13}\text{C}$  NMR (75 MHz,  $\text{CDCl}_3$ )  $\delta$  198.54, 158.67, 149.63, 145.91, 132.33, 120.87, 116.11, 60.49, 58.99, 36.37, 23.41. Mass spectrum ( $\text{EI}^+$ , 70 eV)  $m/z$  192 (100%), 177 (34%), 149 (9%), 107 (9%), 91 (6%), 77 (7%).

A 50 ml two-necked flask equipped with condenser and nitrogen line was charged with 4,5-dimethoxy-1-indanone, 1.5 g (7.80 mmol), and NaCN, 1.91 g (0.038 mol), dissolved in 15 ml of dry DMSO and heated in an oil bath to  $160^\circ\text{C}$  with vigorously stirring for 20 h. The dark brown reaction mixture was quenched with 150 ml  $\text{H}_2\text{O}$ , the aqueous layer extracted 4× with ether, and the combined organic layer dried with anhydrous  $\text{Na}_2\text{SO}_4$  and concentrated *in vacuo* to a dark oil. *E*-Indanone, 5-hydroxy-4-methoxy-1-indanone, was obtained as yellow crystals in 71% yield after column chromatography ( $\text{SiO}_2$ , 9:1, hexane/EtOAc).  $^1\text{H}$  NMR (300 MHz,  $\text{CDCl}_3$ )  $\delta$  7.49 (d, 1H, J = 8.2 Hz, aromatic), 7.00 (d, 1H, J = 8.2 Hz, aromatic), 6.36 (s, 1H, -OH), 4.01 (s, 3H, - $\text{OCH}_3$ ), 3.20 (t, 2H, J = 5.7 Hz, - $\text{CH}_2$ -), 2.71 (t, 2H, J = 6.0 Hz, - $\text{CH}_2$ -).  $^{13}\text{C}$  NMR (500 MHz,  $\text{CDCl}_3$ )  $\delta$  204.70, 154.01, 145.28, 143.12, 131.21, 120.70, 115.95, 60.25, 36.20, 23.23. Mass spectrum ( $\text{EI}^+$ , 70 eV)  $m/z$  178 ( $\text{M}^+$ , 100%), 163 (50%), 135 (21%), 107 (28%), 91 (23%), 77 (16%).

*5-Hydroxy-6-methoxy-1-indanone (Z-indanone)*. Demethylation of 5,6-dimethyl-1-indanone followed the same course as the *E*-indanone to yield a pure yellowish oil in 67% yield.  $^1\text{H}$  NMR (300 MHz,  $\text{CDCl}_3$ )  $\delta$  7.21 (s, 1H, aromatic), 6.98 (s, 1H, aromatic), 6.23 (s, 1H, -OH), 3.95 (s, 3H, - $\text{OCH}_3$ ), 3.05 (t, 2H, J = 5.27 Hz, - $\text{CH}_2$ -), 2.68 (t, 2H, J = 5.83 Hz, - $\text{CH}_2$ -).  $^{13}\text{C}$  NMR (500 MHz,  $\text{CDCl}_3$ )  $\delta$  205.95, 152.42, 150.92, 146.83, 129.59, 111.10, 104.02, 56.16, 36.45, 25.38. Mass Spectrum ( $\text{EI}^+$ , 70 eV)  $m/z$  178 ( $\text{M}^+$ , 100%), 163 (62%), 135 (16%), 107 (24%), 91 (52%), 77 (18%), 63 (9%), 55 (7%).

### Bacterial strains and media

*E. coli* strain DH5 $\alpha$  (Gibco) was used as recipient of plasmids from all cloning manipulations. These plasmids were then isolated and transferred to *A. tumefaciens*, using electroporation, as necessary. *A. tumefaciens* strains: A348 [65] has the C58 chromosomal background with pTiA6; 358mx [55] is an A348 derivative harboring insertion of the transposon Tn3-HoHo1 in the *virE2* gene of pTiA6 creating a *virE::lacZ* fusion. UIA143 [66] is strain C58 lacking its Ti plasmid and carrying an erythromycin resistance gene in the chromosomal *recA* gene. Strains AB140–148 are phenolic hypersensitive mutants, derived from strain A348 as described below.

**Table 2**

Plasmids.		
Plasmid	Relevant characteristics	Source or reference
pAC1	NPTII structural gene ( <i>nptII</i> ) from pCamVNeo as a <i>Bam</i> HI fragment cloned into <i>Bam</i> HI site of pED32, Tet <sup>R</sup>	This study
pAC2	<i>virB<sup>P</sup>/nptII</i> from pAC1, as a <i>Hind</i> III fragment, cloned into pMON596;Spec <sup>R</sup> , IncP	This study
pCamVNeo	pUC8 derivative containing the <i>nptII</i> coding sequences on a 1.0 kb <i>Bam</i> HI fragment	[68,72]
pCF218	<i>traR</i> expressed constitutively from <i>tetR</i> -promoter; cloned into pSW213, Tet <sup>R</sup> , IncP	[73]
pED32A	<i>virB</i> promoter expression vector;Tet <sup>R</sup> , Amp <sup>R</sup> , Spec <sup>R</sup> , IncP	[53]
pMON596	binary vector; carries the 19S-hygromycin resistance gene; Spec <sup>R</sup> ; IncP; derived from pMON574	[74]
pSW209	IncP, <i>virB::lacZ</i> fusion derived from pSM243cd, Kan <sup>R</sup>	S.C. Winans, unpublished

Strains were maintained on LB plates or AB minimal medium [67] supplemented with antibiotics as appropriate. AB induction medium (ABIM), pH 5.5 and containing 1% glucose or 1% glycerol +/- 0.1% arabinose, was used for *vir* gene expression studies. The plasmids used in this study are listed in Table 2.

#### *pAC2* construction

The *Bam*HI fragment from pCamVNeo [68], which contains the coding sequence of *nptII*, was cloned into the *Bam*HI site of pED32, a plasmid that contains the *virB* promoter with a multiple cloning site [53]. This yielded pAC1, a plasmid that had *nptII* expression driven by the inducible *virB* promoter (*virB<sup>P</sup>/nptII*), with tetracycline resistance as its antibiotic marker. The *Hind*III fragment carrying the *virB<sup>P</sup>/nptII* construct was removed from pAC1 and inserted into the *Hind*III site of pMON596.

#### *Vir* induction assay

*A. tumefaciens* strains were grown overnight at 27°C to an optical density of ~0.3–0.6 at 600 nm (OD<sub>600</sub>) in LB medium supplemented with appropriate antibiotics. Cells were then pelleted by centrifugation and resuspended to an OD<sub>600</sub> of 0.1 per ml in sterilized induction medium (ABIM, pH 5.5) supplemented with either 1% glucose or 1% glycerol with or without 0.1% arabinose (w/v). The various phenolic compounds tested were dissolved in a minimal amount of DMSO in water as mM stocks, and diluted with ABIM to the desired concentration (final DMSO concentration was no greater than 0.1%). The bacteria were incubated with at 25°C for 8–16 h and subsequently assayed for β-galactosidase activity by the method of Miller [69]. ED<sub>50</sub> values for the inducers evaluated were estimated from such dose response plots. Each assay value reported is the mean of three replicates; error bar indicates one standard deviation from the mean. Data are representative of three similar independent experiments.

#### Mutant selection

Preliminary experiments indicated that *A. tumefaciens* strain A348/pAC2, grown on induction plates plus 40 μg/ml kanamycin survive at 100 μM AS but are killed at 30 μM AS, demonstrating the

phenolic induction of kanamycin resistance is provided by pAC2 (vector controls died at all AS concentrations). Phenolic hypersensitive mutants were selected as follows. Individual colonies of A348/pAC2 were grown overnight in LB broth plus spectinomycin, and the progeny from each colony kept separate to ensure that each mutation was an individual event, not part of a clonal population. The bacteria were subsequently washed in ABIM medium, resuspended to an OD<sub>600</sub> of approximately 0.1 and induced overnight in ABIM media plus 100 μM AS. The next day the cells had grown to an approximate OD<sub>600</sub> of 1.0 and 2 × 10<sup>5</sup> to 2 × 10<sup>6</sup> bacteria were plated onto plates containing ABIM medium containing 10 μM AS and 40 μg/ml kanamycin. Colonies that grew on this selection medium were subsequently assayed for growth on plates containing kanamycin but no phenolic. Colonies that grew under these conditions are constitutive for kanamycin resistance and were not characterized further, but colonies that couldn't survive in this screen were characterized further.

The kanamycin-resistance test of selected colonies in response to different doses of phenol was done in the following manner: after one night of induction in ABIM over a range of inducer concentrations, as described above, the bacteria were washed and subcultured into ABIM at a starting OD<sub>600</sub> of ~0.1. The ABIM included phenolics at a range of concentrations between 0.1 and 1000 μM. At each concentration of inducer, three cultures have kanamycin at a concentration of 20 μg/ml, while one culture has no kanamycin. After overnight culture the OD<sub>600</sub> is determined and kanamycin-resistant growth as a percentage of control is determined using the following calculation:

$$\% \text{ growth} = \frac{(\text{OD}_{600} \text{ overnight culture} + \text{kanamycin}) \times 100}{(\text{OD}_{600} \text{ overnight culture w/no kanamycin})}$$

The mean of three samples is then plotted versus log of concentration of inducer.

#### Immunoblot

Cultures of different strains were induced overnight in ABIM containing 1% glycerol and 0.1% arabinose and varying phenolic concentrations. Samples from each culture, containing an equivalent OD<sub>600</sub>, were denatured by boiling in sample buffer for 3–10 minutes, and 10 μl from each sample was loaded onto 10% acrylamide gels and separated using SDS–polyacrylamide gel electrophoresis (PAGE). Proteins were transferred from the acrylamide gel to nitrocellulose purchased from Schleicher and Schell (Keene, NH) by electrotransfer. VirB10 expression was examined using immunoblot procedures and antibodies described in Beaupré *et al.* [70].

#### Virulence assays

The capacity of various strains of *A. tumefaciens* to induce tumors on leaf explants of *Nicotiana tabacum* cv Havana 425 was tested as described previously [16].

#### Ti plasmid conjugation

Conjugal transfer of pTiA6 from either the wild type or hypersensitive strains to strain UIA143/pSW209 was carried out as described by Bohne *et al.* [71].

#### Note added in proof

Recent studies by Lohrke *et al.* (Lohrke, S.M., Nechaev, S., Yang, H., Severinov, K. & Jin, S.J. (1999). Transcriptional activation of *Agrobacterium tumefaciens* virulence gene promoters in *Escherichia coli* requires the *A. tumefaciens* *rhoA* gene, encoding the α subunit of RNA polymerase. *J. Bacteriol.* **181**, 4533–4539) support the model that genetic elements outside of VirA and VirG are necessary for *vir* gene expression.

#### Acknowledgements

We thank S.C. Winans (Cornell University) for providing pSW209, Marco Orlandi (University of Milano-Bicocca) for providing a synthetic sample of (2S,3S)-(–)-*trans*-DDF for comparison, and NIH GM47369 for support.

## References

- Zupan, J.R. & Zambryski P. (1995). Transfer of T-DNA from Agrobacterium to the plant cell. *Plant Physiol.* **107**, 1041-1047.
- Hooykaas, P.J.J. & Beijersbergen A.G.M. (1994). The virulence system of *Agrobacterium tumefaciens*. *Annu. Rev. Phytopathol.* **32**, 157-179.
- Christie, P.J. (1997). *Agrobacterium tumefaciens* T-complex transport apparatus: a paradigm for a new family of multifunctional transporters in eubacteria. *J. Bacteriol.* **179**, 3085-3094.
- Birch, R.G. (1997). Plant transformation: problems and strategies for practical application. *Annu. Rev. Plant Physiol.* **48**, 297-326.
- Winans, S.C. (1992). 2-way chemical signaling in Agrobacterium-plant interactions. *Microbiol. Rev.* **56**, 12-31.
- Pirrung, M.C. (1999). Histidine kinases and two-component signal transduction systems. *Chem. Biol.* **6**, R167-R175.
- McEvoy, M.M. & Dahlquist, F.W. (1997). Phosphohistidines in bacterial signaling. *Curr. Opin. Struct. Biol.* **7**, 793-797.
- Heath, J.D., Charles, T.C. & Nester, E.W. (1995). Ti plasmid and chromosomally encoded two-component systems important in plant cell transformation by *Agrobacterium* species. In *Two-Component Signal Transduction*. (Hoch, J.A. & Silhavy, T.J., eds.), pp. 367-385. ASM Press, Washington, D.C.
- Swanson, R.V., Alex, L.A. & Simon, M.I. (1994). Histidine and aspartate phosphorylation: two-component systems and the limits of homology. *Trends Biochem. Sci.* **19**, 485-490.
- Parkinson, J.S. & Kofoed, E.C. (1992). Communication modules in bacterial signaling proteins. *Ann. Rev. Genet.* **26**, 71-112.
- Parkinson, J.S. (1993). Signal transduction schemes of bacteria. *Cell* **73**, 857-871.
- Melchers, L.S., Regensburg-Tuink, T.J.G., Bourret, R.B., Sedee, N.J.A., Schilperoord, R.A. & Hooykaas, P.J.J. (1989). Membrane topology and functional analysis of the sensory protein VirA of *Agrobacterium tumefaciens*. *EMBO J.* **8**, 1919-1925.
- Turk, S.C.H.J., Melchers, L.S., den Dulk-Ras, H., Regensburg-Tuink, A.J.G., & Hooykaas, P.J.J. (1991). Environmental conditions differentially affect *vir* gene induction in different *Agrobacterium* strains. Role of the VirA protein. *Plant Mol. Biol.* **16**, 1051-1059.
- Cangelosi, G.A., Ankenbauer, R.G., & Nester, E.W. (1990). Sugars induce the *Agrobacterium* virulence genes through a periplasmic binding protein and a transmembrane signal protein. *Proc. Natl. Acad. Sci. USA* **87**, 6708-6712.
- Shimoda, N., Toyoda, Y.A., Nagamine, J., Usami, S., Katayama, M., Sakagami, Y. & Machida, Y. (1990). Control of expression of *Agrobacterium vir* gene by synergistic actions of phenolic signal molecules and monosaccharides. *Proc. Natl. Acad. Sci. USA* **87**, 6684-6688.
- Banta, L.M., Joerger, R.D., Howitz, V.R., Campbell, A.M., & Binns, A.N. (1994). Glu-255 outside the predicted ChvE binding site in VirA is crucial for sugar enhancement of aceto-syringone perception by *Agrobacterium tumefaciens*. *J. Bacteriol.* **176**, 3242-3249.
- Turk, S.C.H., van Lange, R.P., Sonneveld, E., & Hooykaas, P.J.J. (1993). The chimeric VirA-Tar receptor protein is locked into a highly responsive state. *J. Bacteriol.* **175**, 5706-5709.
- Machida, Y., *et al.*, & Obata, R.T. (1993). Molecular interactions between *Agrobacterium* and plant cells. p. 85-96. In E.W. Nester and D.P.S. Verma (eds.), *Advances in molecular genetics of plant-microbe interactions*, Kluwer Academic Publishers, The Netherlands.
- Chang, C.H. & Winans, S.C. (1992). Functional roles assigned to the periplasmic, linker, and receiver domains of the *Agrobacterium tumefaciens* VirA protein. *J. Bacteriol.* **174**, 7033-7039.
- Doty, S.L., Yu, M.C., Lundin, J.I., Heath, J.D. & Nester E.W. (1996). Mutational analysis of the input domain of the VirA protein of *Agrobacterium tumefaciens*. *J. Bacteriol.* **178**, 961-970.
- Turk, S.C.H.J., Vanlange, R.P., Regensburgtuink T.J.G. & Hooykaas P.J.J. (1994). Localization of the VirA domain involved in acetosyringone-mediated *vir* gene induction in *Agrobacterium tumefaciens*. *Plant Mol. Biol.* **25**, 899-907.
- Chang, C.H., Zhu, J. & Winans, S.C. (1996). Pleiotropic phenotypes caused by genetic ablation of the receiver module of the *Agrobacterium tumefaciens* VirA protein. *J. Bacteriol.* **178**, 4710-4716.
- Lee, Y.W., Jin, S., Sim, W.S. & Nester E.W. (1995). Genetic evidence for direct sensing of phenolic compounds by the VirA protein of *Agrobacterium tumefaciens*. *Proc. Natl. Acad. Sci. USA* **92**, 12245-12249.
- Peng, W.T., Lee, Y.W. & Nester, E.W. (1998). The phenolic recognition profiles of the *Agrobacterium tumefaciens* VirA protein are broadened by a high level of the sugar binding protein ChvE. *J. Bacteriol.* **180**, 5632-5638.
- Lee, K.H., Dudley, M.W., Hess, K.M., Lynn, D.G., Joerger, R.D. & Binns, A.N. (1992). Mechanism of activation of *Agrobacterium* virulence genes – identification of phenol-binding proteins. *Proc. Natl. Acad. Sci. USA* **89**, 8666-8670.
- Dye, F. & Delmotte, F.M. (1997). Purification of a protein from *Agrobacterium tumefaciens* strain A348 that binds phenolic compounds. *Biochem. J.* **321**, 319-324 Part 2.
- Duban, M.E., Lee, K.H. & Lynn D.G. (1993). Strategies in pathogenesis – mechanistic specificity in the detection of generic signals. *Mol. Microbiol.* **7**, 637-645.
- Melchers, L.S., Regensburgtuink, A.J.G., Schilperoord, R.A. & Hooykaas, P.J.J. (1989). Specificity of signal molecules in the activation of *Agrobacterium* virulence gene expression. *Mol. Microbiol.* **3**, 969-977.
- Spencer, P.A. & Towers, G.H.N. (1988). Specificity of signal compounds detected by *Agrobacterium tumefaciens*. *Phytochemistry* **27**, 2781-2785.
- Teutonico, R., Dudley, M.D., Orr, J.D., Lynn, D.G. & Binns, A.W. (1991). Activity and accumulation of cell-division-promoting phenolics in tobacco. *Plant Physiol.* **97**, 288-297.
- Orr, J.D., Dudley, M.D. & Lynn, D.G. (1992). Biosynthesis of the dehydrodiconiferyl glucosides: implications for the control of tobacco cell growth. *Plant Physiol.* **98**, 343-352.
- Lynn, D.G., Chen, R.H., Manning, K.S., & Wood, H.N. (1987). The structural characterization of endogenous factors from *Vinca rosea* L. crown gall tumors which promote cell division in tobacco cells. *Proc. Natl. Acad. Sci. USA* **84**, 615-619.
- Binns, A., Chen, R.H., Wood, H.N., & Lynn, D.G. (1987). Cell division promoting activity of naturally occurring dehydrodiconiferyl glucosides: do cell wall components control cell division? *Proc. Natl. Acad. Sci. USA* **84**, 980-984.
- Tamagnone, L., *et al.*, & Martin, C. (1998). Inhibition of phenolic acid metabolism results in precocious cell death and altered cell morphology in leaves of transgenic tobacco plants. *Plant Cell* **10**, 1801-1816.
- Dudley, M. (1991). *Synthetic Probes of Signal Transduction Pathways* [Ph.D. thesis]. The University of Chicago, Chicago.
- Hirai N., Okamoto M., Udagawa H., Yamamuro M., Kato M. & Koshimizu K. (1994). Absolute configuration of dehydrodiconiferyl alcohol. *BioSci. Biotech. Biochem.* **58**, 1679-1684.
- Aratani, T. (1985). Catalytic asymmetric synthesis of cyclopropane-carboxylic acids: an application of chiral copper carbenoid reaction. *Pure Appl. Chem.* **57**, 1839-1844.
- Noyori, R. (1990). Chiral metal complexes as discriminating molecular catalysts. *Science* **248**, 1194-1199.
- Salomon, R.G. & Kochi, J.K. (1973). Copper(I) catalysis in cyclopropanation with diazo compounds, the role of olefin coordination. *J. Am. Chem. Soc.* **95**, 3300-3310.
- Lownthal, R.E., Abiko, A. & Masamune S. (1990). Asymmetric catalytic cyclopropanation of olefins: Bis-oxazoline copper complexes. *Tetrahedron Lett.* **31**, 6005-6008.
- Lownthal, R.E. & Masamune S. (1991). Asymmetric copper-catalyzed cyclopropanation of trisubstituted and unsymmetrical *cis*-1,2-disubstituted olefins: modified bis-oxazoline ligands. *Tetrahedron Lett.* **32**, 7373-7376.
- Evans, D.E., Woerpel, K.A., Hinman, M.M. & Faul, M.M. (1991) Bis(oxalines) as chiral ligands in metal-catalyzed asymmetric reactions. Catalytic, asymmetric cyclopropanation of olefins. *J. Am. Chem. Soc.* **113**, 726-728.
- Evans, D.E., Woerpel K.A. & Scott M.J. (1992) 'Bis(oxalines)' as ligands for self-assembling chiral coordinates polymers-structure of a copper(I) catalysts for the enantioselective cyclopropanation of olefins. *Angew. Chem. Int. Ed. Engl.* **31**, 430-432.
- Harada, N. & Nakanishi, K. (1972). The exciton chirality method and its application to configurational and conformation studies of natural products. *Accounts Chem. Res.* **8**, 257-263.
- Harada, N. & Nakanishi, K. (1983). *Circular Dichroic Spectroscopy-Exciton Coupling in Organic Stereochemistry*. University Science Books, Mill Valley.
- Charette, A.B. & Juteau, H. (1994). Design of amphoteric bifunctional ligands: application to the enantioselective Simmons-Smith cyclopropanation of allylic alcohols. *J. Am. Chem. Soc.* **116**, 2651-2652.
- Charette, A.B., Prescott, S. & Brochu C. (1995). Improved procedure for the synthesis of enantiomerically enriched cyclopropylmethanol derivatives. *J. Org. Chem.* **60**, 1081-1083.
- Theberge, C.R., Verbicky C.A. & Zercher, C.K. (1996). Studies on the diastereoselective preparation of bis-cyclopropanes. *J. Org. Chem.* **61**, 8792-8798.

49. Simmons, H.E. & Smith, R.D. (1958). A new synthesis of cyclopropanes from olefins. *J. Am. Chem. Soc.* **80**, 5323-5324.
50. Simmons, H.E. & Smith, R.D. (1959). A new synthesis of cyclopropanes. *J. Am. Chem. Soc.* **81**, 4256-4264.
51. Furukawa, J., Kawabata, N. & Nishimura, J. (1966). A novel route to cyclopropanes from olefins. *Tetrahedron Lett.* 3353-3354.
52. Furukawa, J., Kawabata, N. & Nishimura, J. (1968). Synthesis of cyclopropanes by the reaction of olefins with dialkylzinc and methylene iodide. *Tetrahedron* **24**, 53-58.
53. Ward, J.E., Dale, E.M., Christie, P.J., Nester, E.W. & Binns, A.N. (1990). Complementation analysis of *Agrobacterium tumefaciens* Ti plasmid *virB* genes by use of a *vir* promoter expression vector – *virB9*, *virB10*, and *virB11* are essential virulence genes. *J. Bacteriol.* **172**, 5187-5199.
54. Klee, H.J., White, F.F., Iyer, V.N., Gordon, M.P. & Nester, E.W. (1983). Mutational analysis of the virulence region of an *Agrobacterium tumefaciens* Ti plasmid. *J. Bacteriol.* **153**, 878-883.
55. Stachel, S.E. & Nester, E.W. (1986). The genetic and transcriptional organization of the *vir* region of the A6-Ti plasmid of *Agrobacterium tumefaciens*. *EMBO J.* **5**, 1445-1454.
56. Pazour, G.J., Ta, C.N. & Das, A. (1991). Mutants of *Agrobacterium tumefaciens* with elevated *vir* gene expression. *Proc. Natl Acad. Sci. USA* **88**, 6941-6945.
57. Ankenbauer, R.G., Best, E.A., Palanca, C.A. & Nester, E.W. (1991). Mutants of the *Agrobacterium tumefaciens virA* gene exhibiting acetosyringone-independent expression of the *vir* regulon. *Mol. Plant Microbe Interact.* **4**, 400-406.
58. Mclean, B.G., Greene, E.A. & Zambryski, P.C. (1994). Mutants of *Agrobacterium VirA* that activate *vir* gene-expression in the absence of the inducer acetosyringone. *J. Biol. Chem.* **269**, 2645-2651.
59. Hess, K., Dudley, M.D., Lynn, D.G., Joerger, R.D. & Binns, A. (1991). Mechanism of phenolic activation of *Agrobacterium* virulence genes: Development of a specific inhibitor of bacterial sensor/response systems. *Proc. Natl Acad. Sci. USA* **88**, 7854-58.
60. Pellequer, J-L., Brudler, R. & Getzoff, E. D. (1999). Biological sensors: more than one way to sense oxygen. *Curr. Biol.* **9**, R416-R418.
61. Gong, W., Hao, B., Mansy, S.S., Gonzalez, G., Gilles-Gonzalez, M.A. & Chan, M.K. (1998). Structure of a biological oxygen sensor: a new mechanism for heme-driven signal transduction. *Proc. Natl Acad. Sci. USA* **95**, 15177-15182.
62. Shimoda, N., Toyoda, Y.A., Aoki, S. & Machida, Y. (1993). Genetic evidence for an interaction between the VirA sensor protein and the ChvE sugar-binding protein of *Agrobacterium*. *J. Biol. Chem.* **268**, 26552-26558.
63. Wanner, B.L. (1993). Gene regulation by phosphate in enteric bacteria. *J. Cell. Biochem.* **51**, 47-53.
64. Shi, L. & Hulett, F.M. (1999) The cytoplasmic kinase domain of PhoR is sufficient for the low phosphate-inducible expression of Pho regulon genes in *Bacillus subtilis*. *Mol. Microbiol.* **31**, 211-222.
65. Garfinkel, D.J., Simpson, R.B., Ream, L.W., White, F.F., Gordon, M.P. & Nester, E.W. (1981). Genetic analysis of crown gall: fine structure map of the T- DNA by site-directed mutagenesis. *Cell* **27**, 143-153.
66. Farrand, S.K., Omorchoe, S.P., Mccutchan, J. (1989). Construction of an *Agrobacterium tumefaciens c58 recA* mutant. *J. Bacteriol.* **171**, 5314-5321.
67. Winans, S.C., Kerstetter R.A. & Nester, E.W. (1988). Transcriptional regulation of the *virA*-Gene and *virG*-Gene of *Agrobacterium tumefaciens*. *J. Bacteriol.* **170**, 4047-4054.
68. Fromm, M.E., Taylor, L.P. & Walbot, V. (1986). Stable transformation of maize after gene transfer by electroporation. *Nature* **319**, 791-793.
69. Miller, J.H. (1972). *Experiments in molecular genetics*. Cold Spring Harbor Laboratory, Cold Spring Harbor, N.Y.
70. Beaupré, C.E., Bohne, J., Dale, E.M. & Binns A. N. (1997). Interactions between VirB9 and VirB10 membrane proteins involved in movement of DNA from *Agrobacterium tumefaciens* into plant cells. *J. Bacteriol.* **179**, 78-89
71. Bohne, J., Yim, A., Binns, A.N. (1998). The Ti plasmid increases the efficiency of *Agrobacterium tumefaciens* as a recipient in *virB*-mediated conjugal transfer of an IncQ plasmid. *Proc. Natl Acad. Sci. USA* **95**, 7057-7062.
72. Beck, E., Ludwig, G., Auerswald, E.A., Reiss, B. & Schaller, H. (1982). Nucleotide-sequence and exact localization of the neomycin phosphotransferase gene from transposon tn5. *Gene* **19**, 327-336.
73. Fuqua, W.C. & Winans, S.C. (1994). A luxR-luxI type regulatory system activates *Agrobacterium* Ti plasmid conjugal transfer in the presence of a plant tumor metabolite. *J. Bacteriol.* **176**, 2796-2806.
74. Ma, H., Yanofsky, M.F., Klee, H.J., Bowman, J.L., Meyerowitz, E.M. (1992). Vectors for plant transformation and cosmid libraries. *Gene* **117**, 161-167.

---

**Because Chemistry & Biology operates a 'Continuous Publication System' for Research Papers, this paper has been published via the internet before being printed. The paper can be accessed from <http://biomednet.com/cbiology/cmb> – for further information, see the explanation on the contents pages.**